Published in final edited form as:
J Neurosci. 2010 December 8; 30(49): 16609–16620. doi:10.1523/JNEUROSCI.3695-10.2010.

Specific brainstem neurons switch each other into pacemaker mode to drive movement by activating NMDARs

W.-C. Li[1,2], **A. Roberts**[2], and **S. R. Soffe**[2]

[1] School of Biological Sciences, University of St Andrews, Bute, St Andrews, UK

[2] School of Biological Sciences, University of Bristol, Bristol, BS8 1UG, UK.

Abstract

Rhythmic activity is central to brain function. In the vertebrate central nervous system, the neuronal circuits for breathing and locomotion involve inhibition and also neurons acting as pacemakers, but identifying the neurons responsible has proven difficult. By studying simple hatchling *Xenopus laevis* tadpoles, we have already identified a population of electrically coupled hindbrain neurons (dINs) which drive swimming. During rhythm generation dINs release glutamate to excite each other and activate NMDA receptors (NMDARs). The resulting depolarization enables a network mechanism for swimming rhythm generation which depends on reciprocal inhibition between antagonistic right and left sides. Surprisingly, a surgically isolated hemi-CNS without inhibition can still generate swimming-like rhythms. We have now discovered that activation of NMDARs transforms dINs, which normally fire singly to current injection, into pacemakers firing within the normal swimming frequency range (10-25 Hz). When dIN firing is blocked pharmacologically, this NMDAR activation produces 10 Hz membrane potential oscillations which persist when electrical coupling is blocked but not when the voltage-dependent gating of NMDARs by Mg^{2+} is removed. The NMDA-induced oscillations and pacemaker firing at swimming frequency are unique to the dIN population and do not occur in other spinal neurons. We conclude that NMDAR-mediated self-resetting switches critical neurons which drive swimming into pacemaker mode only during locomotion where it provides an additional, parallel mechanism for rhythm generation. This allows rhythm generation in a half CNS and raises the possibility that such concealed pacemaker properties may be present underlying rhythm generation in other vertebrate brain networks.

Keywords

Locomotion; swimming; interneuron; NMDAR; pacemaker; rhythm; central pattern generator; spinal cord

Introduction

Rhythmic activity is widespread in the vertebrate central nervous system controlling functions like locomotion, respiration, sleep and memory consolidation (for reviews see e.g. (Buzsaki and Draguhn, 2004; Ramirez et al., 2004)). Rhythm generating networks rely on both the synaptic connections between network neurons and the cellular properties of the neurons (Getting, 1989; Harris-Warrick, 2002; Arshavsky, 2003; Ramirez et al., 2004; Guertin, 2009; Brocard et al., 2010). Vertebrate locomotion requires rhythmic patterned activation of trunk and limb muscles. Although spinal networks can organize such

correspondence wl21@st-andrews.ac.uk.

Europe PMC Funders Author Manuscripts

locomotor rhythms, it is generally assumed that descending excitation from hindbrain reticulospinal neurons is necessary to activate NMDARs and turn on the spinal rhythms (Arshavsky Yu et al., 1984; Atsuta et al., 1990; Noga et al., 1991). To investigate whether pacemaker properties are involved in rhythm generation, TTX has been used in many preparations to block impulses. NMDA induces slow (typically ~1 Hz) membrane potential oscillations in motoneurons and some interneurons which may contribute to their rhythmic firing during locomotion (Grillner and Wallen, 1985; Wallen and Grillner, 1985, 1987; Hochman et al., 1994a; Hochman et al., 1994b; Sillar and Simmers, 1994; Rioult-Pedotti, 1997; Guertin and Hounsgaard, 1998; Reith and Sillar, 1998; Prime et al., 1999; Tresch and Kiehn, 2000; Wilson et al., 2005).

In hatchling *Xenopus* tadpole, we have recently established that one type of reticulospinal neuron (dINs) provides the excitatory synaptic drive to spinal neurons during swimming locomotion. The reliable generation of the swimming rhythm depends: firstly, on dINs exciting each other by releasing glutamate to activate AMPARs and NMDARs; secondly, on rebound firing in the dINs following reciprocal inhibition (Li et al., 2006; Soffe et al., 2009); and thirdly on the dINs being electrically coupled to each other (Li et al., 2009). However, a swimming-like rhythm of motor activity at 15 to 25 Hz can also be produced by a single, surgically isolated side of the CNS (hemi-CNS) even when inhibition is blocked by antagonists (Soffe, 1989). Single sided swimming rhythms have also been found in the lamprey (Cangiano and Grillner, 2003, 2005). Similarly, the pharmacological block of glycinergic transmission doesn't stop the generation of rhythmic activity in either intact cord or hemi-cord preparations in the mouse (Droge and Tao, 1993; Cowley and Schmidt, 1995; Ozaki et al., 1996; Kremer and Lev-Tov, 1997) and adult frog (Rioult-Pedotti, 1997). These results suggest that other, possibly cellular pacemaker mechanisms are present that do not depend on inhibition. Our aim is to reveal pacemaker properties in the tadpole swimming circuit that could contribute to normal network rhythm generation and also allow a single side of the CNS to generate rhythm.

We found that the application of NMDA can indeed transform the reticulospinal dIN neurons that drive swimming into pacemakers. Since dINs synapse with each other and release glutamate to activate NMDARs, this suggests a novel role for NMDAR activation to self-reset the firing properties within a neuronal population while it is in an active state.

Experimental procedures

Preparation

Human chorionic gonadotropin injections were carried out regularly in our *Xenopus* colony to induce mating. Embryos were collected and incubated at different temperatures to alter their developmental rates. All experiment procedures have been approved by local Animal Welfare Ethics committee and comply with UK Home Office regulations. *Xenopus* tadpoles (stage 37/38, (Nieuwkoop and Faber, 1956)) were briefly anaesthetised using 0.1% MS222 (3-aminobenzoic acid ester, Sigma, UK), then immobilised using 12.5 μM α-bungarotoxin (Tocris Cookson, Brisol, UK) and mounted onto a small sylgard stage using fine tungsten pins for dissections as described previously (Li et al., 2002). The saline had the following concentrations in mM: NaCl 115, KCl 3, $CaCl_2$ 2, $NaHCO_3$ 2.4, $MgCl_2$ 1, HEPES 10, adjusted to pH 7.4 with NaOH. Once the CNS was exposed ((Fig.1A, B, C), the hemi-CNS preparation was made by cutting through the cord caudally at the 8^{th} to 9^{th} muscle segment and the hindbrain at the level of the ear vesicle (5^{th} to 6^{th} rhombomere segments). The left side of the hindbrain and spinal cord was then removed between these cuts (Fig.1D). The nervous system was then opened dorsally and tissue removed to expose neuronal somata to allow access of whole-cell recording electrodes.

Recordings

Following dissections, whole-cell current clamp recordings were made from exposed neuronal somata using patch pipettes filled with 0.1% neurobiotin (Vector Labs, Burlingame, CA) in the intracellular solution (concentrations in mM: K-gluconate 100, $MgCl_2$ 2, EGTA 10, Hepes 10, Na_2ATP 3, NaGTP 0.5 adjusted to pH 7.3 with KOH). Pipette had DC resistances ranging from 10 to 20 MΩ. Whole-cell recordings were mostly made using Axon Multiclamp 700B, digitised with Digidata 1440A, sampled with pClamp 10 software (Molecular Devices). Some whole-cell recordings were made with Axon-2B amplifier, CED 1401 plus digitiser and Signal software (Cambridge Electronic Design). Tip potentials were corrected before making recordings. Micorperfusion of NMDA or L-glutamate (Sigma, UK) was done by using a glass pipette with an opening of 10 μm at the tip positioned as close as 30 μm to the recorded soma. To test the effects of NMDA on dIN properties (firing, oscillations), the level of NMDAR activation was adjusted by changing either the perfusion pressure or the distance of the microperfusion pipette from the recorded neuron somata. In this case, the actual concentration of NMDA reaching its sites of action can vary from trial to trial and will be lower than the concentration in the pipette due to dilution with saline. In a few experiments, NMDA or L-glutamate (both at 100 mM prepared with equimolar sodium hydroxide) was applied by microiontophoresis. The microiontophoresis electrodes had DC resistances of 150 – 200 MΩ when filled with 3 M potassium acetate and were placed within 50 μm upstream to the recording site. Pulses of negative current less than 2.5 nA were configured using pClamp10 and injected through the second channel of the MultiClamp 700B. Simply positioning the microiotophoresis electrode close to the recorded neuron did not cause a membrane potential change so holding currents were not used. In immobilised tadpoles fictive swimming was evoked by 1 ms current pulse stimulation to the skin, dimming the microscope light or, in some hemi-CNS preparations, stimulating the hindbrain directly. Motor nerve recordings were made by placing a suction electrode on the segmented swimming muscle clefts to monitor spinal cord outputs. In preparations where tetrodotoxin (TTX, Sigma, UK) or Cd^{2+} was used to block action potential triggered synaptic transmission, the half-hindbrain was left intact so light-dimming could be used to evoke swimming-like rhythms so active dINs could be found using extracellular recording. In many hemi-CNS preparations, NMDA was microperfused onto the caudal hindbrain/rostral spinal cord region to initiate rhythmic activity. Such activity was monitored either by making motor nerve recordings or by recording directly from the caudal hemi-cord using a suction electrode (Fig.1). When 18-β-glycyrrhetinic acid (18-β-GA, Sigma, UK) was used to block the electrical coupling, 100 μM NMDA was bath-applied to induce oscillation. In this case, pairs of dINs were recorded in perforated whole-cell recording mode using amphotericin B (100 μg/ml, Merck4Biosciences, Nottingham, UK) to facilitate stable recordings in both neurons. Electrical coupling coefficient was defined as the percentage of voltage response in the uninjected neuron relative to the response in the injected neuron. Neuronal anatomy revealed by neurobiotin filling was used for final neuronal identification. Transmitter antagonists (full name, receptor type) used included: strychnine (GlyR); SR95531, also called gabazine, (6-imino-3-{4-methoxyphenyl}-1{6H}-pyridazinebutanoic acid hydrobromibe, $GABA_ARs$); NBQX (2,3-dihydroxy-6-nitro-7-sulfamoylbenzo-[f]quinoxaline, AMPAR); D-AP5 (D-(-)-2-amino-5-phosphonopentanoic acid, NMDAR, Tocris Cookson, Bristol, UK) and DHβe (Dihydro-β-erythroidine, nAChRs, Research Biochemicals International, Natick, MA).”

Data analyses

These were carried out with Dataview (v6.1, courtesy of Dr W.J. Heitler in the University of St Andrews) and SPSS. In order to classify neuronal responses to NMDA application in the presence of TTX, autocorrelation was applied to the recordings to extract the oscillation frequency (the inverse of the time (T) to the first autocorrelation peak) and measurements of

the first autocorrelation peak and trough. Cluster analyses using oscillation amplitude, frequency and the difference between the first autocorrelation trough and peak measurements were used to classify neurons using SPSS. Power spectrum analyses were carried out using dIN recordings to compare the frequency composition of the oscillations. Phase plots were used to evaluate the synchronicity of oscillations in the simultaneously recorded dINs. To evaluate rhythmicity of either motor nerve or spinal cord bursts, the records were rectified first. Then a threshold amplitude was set to trigger events and histograms of intervals between these events produced using Dataview. Coefficients of rhythmicity were calculated as: Cr = (a1−a2)/(a1+a2), where a1 and a2 are the sizes of the second peak and first trough of the histogram respectively (Thorn Perez et al., 2009) (Fig. 9B). Similar measurements were made of events triggered by action potentials in whole-cell recordings from individual neurons. Means were compared using *t*-tests unless stated otherwise.

Results

Neurons in the caudal hindbrain were identified as reticulospinal dINs during experiments by their unusually long duration action potentials and single spike per cycle firing during swimming-like activity (Fig.1E, (Li et al., 2006). They typically fired a single action potential at the onset of depolarising current injection even well above threshold (Fig. 2A). They were filled with neurobiotin and the identification confirmed if they possessed a descending ipsilateral axon (Fig.1F). The dINs recorded in this paper shared the same properties, physiology, activity during swimming, and anatomy as dINs and hdINs (hindbrain dINs) already extensively documented (Li et al., 2004; Li et al., 2006; Li et al., 2009; Soffe et al., 2009). Significantly, they typically fire just a single action potential at the onset of a step depolarising current injection, even well above threshold (Fig. 1G, 2A). Only interrupting the depolarization with negative current or synaptic inhibition can make them fire again on rebound (Soffe et al., 2009). However, these dINs do not fire to slowly rising depolarisation. When tested in 8 dINs, slowly rising ramp or 0.5 Hz sinusoidal current injection did not produce spikes even when neurons were depolarised to membrane potentials (−10.5 ± 6.3 mV) well above their firing thresholds measured in response to square current pulses (−30 ± 4.5 mV; Fig. 1G). Firing could still be induced in slowly depolarised dINs on rebound from a negative shift in potential.

NMDA induced repetitive firing to current in reticulospinal dINs

During swimming, reticulospinal dINs in the caudal hindbrain receive glutamatergic excitation from other dINs, which activates both AMPAR and NMDAR and summates to provide a sustained background excitation (Li et al., 2006). Here, we tested whether NMDA application could additionally induce any pacemaker-like properties in dINs.

We examined the effects of NMDAR activation by using a pipette with ~ 10 μm tip opening to microperfuse 100 μM NMDA onto dINs (Fig.1D) with 1 μM strychnine and 20 μM SR95531 in the saline. By adjusting the microperfusion pressure and pipette distance from the recorded cell body, we were able to microperfuse sufficient NMDA to slightly depolarise the membrane potential (typically by 5 ~10 mV). This small depolarisation makes it clear that at the dIN resting potential, NMDARs are not fully blocked by Mg^{2+} (cf (Mayer et al., 1984; Soffe and Roberts, 1989)). Interestingly, when this was done, 15 out of 16 single firing dINs started to fire repetitively in response to current injection (Fig.2B). In 7 dINs a series of currents were injected to investigate the firing frequency range. This was very narrow and lay mainly within the normal tadpole swimming frequency range (7 Hz to 27.4 Hz, mean: 17.8 ± 1.7 Hz, 1 dIN with a wider range of 19 to 44 Hz, Fig. 3B). Bigger NMDA depolarization even without current injection always led to repetitive dIN firing (n=15 dINs) often followed by rhythmic network work activity. To avoid such activity and

test if the NMDA was acting directly on dINs to induce repetitive firing we used 150 μM Cd^{2+} to globally block synaptic transmission and 1 μM strychnine, 20 μM SR95531, 2 μM DHβe, 5 μM NBQX to block specific ionotropic receptors. In this case, NMDA induced dIN firing frequency ranging from 5 to 30 Hz (mean of averages: 16.9 ± 2.6 Hz, n=7 dINs, 1192 spikes analyzed, Fig.2C, 3A). Although dINs were previously shown to corelease ACh along with glutamate (Li et al., 2004), repetitive firing in the presence of the antagonist DHβe demonstrates that nicotinic receptor activation is not necessary for the transformation of dIN firing properties.

Since dINs release glutamate, we microperfused 1 mM L-glutamate while using 1 μM strychnine, 20 μM SR95531, 2 μM DHβe, 5 μM NBQX and 150-200 μM Cd^{2+} to block other ionotropic receptors. When glutamate induced depolarisations were small, dINs started to fire repetitively to injected current. Larger glutamate induced depolarisations made dINs fire repetitively without additional current (Fig.2D). The dIN firing frequencies to glutamate applications (mean of average: 16.4 ± 1.9 Hz, n=5 dINs, 680 spikes analysed) are similar to those seen with NMDA applications (Fig.3A; p=0.74). L-glutamate (n=5) or NMDA (n=1, −0.05 - −2.5 nA) applied by microionophoresis also revealed that repetitive dIN firing can be evoked within less than 200 ms (from microiontophoresis current onset to 1^{st} spike peak: 179 ± 95 ms, shortest: 81 ms, Fig.2E), equivalent to a few swimming cycles. When 50 μM D-AP5 was included in the antagonist cocktail, glutamate induced membrane depolarization was largely blocked and glutamate could not make dINs fire (n=7, Fig.2E), further confirming that the activation of NMDARs rather than other ionotropic or metabatropic GluRs is necessary to induce repetitive dIN firing.

The NMDA induced firing of dINs has two significant features for their possible role as conditional pacemaker neurons in the swim rhythm generator: firstly, the firing rates of dINs in NMDA were restricted and were increased little by increasing current injection, and secondly, the firing rates lay mostly within the natural 10 to 25 Hz range of swimming frequencies seen in the tadpole (Fig. 3B; (Kahn et al., 1982)). In contrast, other spinal neurons which are active during swimming (n = 9) fired repetitively to positive current injections at frequencies up to 200 Hz, which are considerably higher than those of swimming (Fig. 3C; (Sautois et al., 2007)). These neurons also fired repetitively at high frequencies to current injection when their membrane potential was depolarised by microperfused NMDA (Fig. 3C; 5.2-14.4 mV from rest). So, unlike dINs, firing characteristics of other spinal neurons are not noticeably changed by NMDA.

NMDA induced oscillations in reticulospinal dINs

Our next step was to examine what happens in the presence of NMDA to make single-firing dINs into potential pacemakers which fire repetitively within the swimming frequency range. Previous work on embryonic *Xenopus* spinal neurons had revealed NMDA induced fast membrane potential oscillations when action potentials were blocked by TTX (Prime et al., 1999). We therefore used 0.4 μM TTX to exclude spikes and therefore spike-evoked chemical synaptic transmission and then applied NMDA to see if oscillations were induced. Both microperfused and bath-applied NMDA (20 – 100 μM) induced clear membrane potential oscillations in 75/77 dINs recorded (Fig. 4A). When NMDA was applied, the dIN membrane potential depolarised and often passed through a region where oscillations occurred before reaching a depolarised plateau. In these cases, we used negative current injection to bring the membrane potential down to a level where oscillations were present and stable. Lowering the concentration of NMDA by carefully reducing microperfusion pressure or increasing microperfusion distance (see Methods) showed that it was not necessary to limit the depolarisation by negative current injection for oscillations to be produced (n = 21 dINs examined).”

The TTX-resistant oscillations were seen over a wide range of membrane potentials. Broadly, the peak-to-trough amplitude of the oscillations was biggest at membrane potentials between −25 and −30 mV, when amplitude could reach >30 mV, and became smaller when the membrane potential was either more or less negative than this (Fig. 4C, n= 6 dINs). Oscillation frequency changed very little when current injection was used to set membrane potential (Fig. 4D), typically varying less than 1Hz over a 100 mV range (linear regression coefficients: 0.008 ± 0.015 Hz/mV, n=5 dINs). This insensitivity of frequency to membrane potential was very similar to that reported for presumed motoneurons by Prime et al. (1999).

The observation that membrane potential oscillations were reliably evoked by NMDA in the presence of TTX suggested that fast sodium channels are not essential for their generation. From a wide range of previous studies, and the membrane potential range where their amplitude was largest, it seemed very likely that the voltage-dependent unblock and block of NMDARs by Mg^{2+} could contribute to the oscillations. When Mg^{2+} was removed from the saline (containing the inhibitory transmitter blockers 1 μM strychnine and 20 μM SR95531), NMDA application sufficient to produce a small depolarisation below dIN firing threshold (around −28 mV, (Sautois et al., 2007)) was no longer able to transform single-firing dINs to repetitive firing in response to depolarising current (n=10; Fig. 5A, C). When the NMDAR depolarization was above dIN firing threshold, dINs in 0 Mg^{2+} saline also failed to fire repetitively in contrast to those in saline with 1 mM Mg^{2+} (n=9, Fig. 5B, D). When TTX was present, NMDA application in 0 Mg^{2+} saline depolarised dINs but no longer produced oscillations of membrane potential (n=6) despite varying the membrane potential over a wide range using current injection (Fig. 5E). These observations suggested that the voltage-dependent Mg^{2+} block of NMDARs plays a critical role in the generation of NMDA-induced oscillations and pacemaker firing in dINs.

To determine if other spinal neurons which are active during swimming showed similar TTX resistant NMDA-induced oscillations we examined the activity of 31 non-dIN neurons (13 motoneurons and 18 non-dIN interneurons) following the microperfusion of 100 μM NMDA in the presence of TTX. To produce comparable activation of receptors in different cell types, we adjusted the perfusion of NMDA to produce similar levels of depolarisation. Generally, closer and higher pressure NMDA perfusion was needed in the non-dINs than in dINs. Some of these neurons (7 motoneurons and 4 non-dIN interneurons) responded with a sustained depolarization and an increasingly noisy membrane potential but no sign of oscillations (Fig.6A). The remaining 20 neurons showed some form of oscillatory response (Fig. 6B, C). However, their oscillatory responses appeared to differ significantly from those in dINs and so the two were compared in detail.

To compare NMDA induced oscillations autocorrelation analyses were applied to activity from 21 dINs and the 20 other spinal neurons showing some oscillatory response. We measured: the main oscillation period (P) and converted this to frequency; the stability of the oscillation (the difference between the first autocorrelation peak and trough Fig. 6D); and mean oscillation amplitude. Cluster analyses using the three measures resolved three groups of neuron (Fig. 6E). 21 dINs formed a single cluster characterised by ~10 Hz oscillations of high amplitude (9.6 ± 2.1 Hz, 34.0 ± 9.4 mV). This cluster also contained a single motoneuron, although the oscillations in this motoneuron were rather slower and weaker than most of the dINs in the same cluster (6.9 Hz, 7.2 mV). A second cluster contained 2 motoneurons and 6 interneurons and was characterised by a much lower oscillation frequency than the dINs but a high amplitude (2.2 ± 1.1 Hz, 27.4 ± 10.0 mV, Fig. 6B). A third cluster containing 3 motoneurons and 7 interneurons had relatively weak ~ 5 Hz oscillations (5.2 ± 2.6 Hz, 6.2 ± 4.3 mV, Fig. 6C). A single interneuron with unreliable oscillations at much higher frequency (47.5 Hz, 29 mV) was close to the dIN cluster but

formed a lone dendrogram branch (asterisk, Fig. 6E). The oscillations shown by the dIN group (including the single motoneuron) were significantly different in most measured parameters from the other two groups (Fig. 6F).

Overall this analysis shows that reliable, strong (~10 Hz) membrane potential oscillations in the presence of NMDA are almost exclusively a feature of dINs, and not of other spinal neuron types (summarised in Fig. 6G). At ~10Hz, these oscillations lie at the lower end of the normal range of swimming frequencies in the hatchling tadpole. The variability of dIN oscillations, reflected in the distances between individual cells of the dIN cluster in the dendrogram, appears to be smaller than for the other two groupings.

Effects of a gap junction blocker on NMDA induced oscillations

An important factor to consider is that the dINs form an electrically coupled population. Gap junctions and electrical coupling play a role in neuronal network rhythm generation and membrane potential oscillations in many other systems. We recently reported electrical coupling between dINs in the tadpole (Li et al., 2009). It was therefore important to explore the significance of this electrical coupling in TTX-resistant NMDA induced oscillations in dINs. In this same recent study, we assessed a range of gap junction blockers in the tadpole and found 40 μM 18-ß-GA to provide the best combination of potency and specificity. 18-β-GA was therefore used to block the electrical coupling in 5 simultaneous recordings from 10 dINs. In order to maintain long and stable whole-cell recordings, the perforated patch-clamp method was employed. Simultaneous recordings allowed us to monitor directly the timing and effectiveness of electrical coupling block. 18-β-GA reduced coupling coefficients from 8 ± 3.2% to 1.6 ± 0.3% (78% block) after application for about 30 minutes. When the electrical coupling block stabilized, the ability of dINs to generate TTX-resistant ~10 Hz oscillations to bath-applied NMDA persisted (Fig. 7A). However, synchronisation between the simultaneously recorded dIN pairs was significantly weakened in 18-β-GA, (Fig. 7B). Cross-correlation analysis showed that NMDA-induced oscillations were highly regular and synchronized in control (peak cross-correlation coefficients: 0.88 ± 0.07, n=5 pairs). In 18-β-GA, cross-correlation peak coefficients fell significantly (0.51 ± 0.15; n=5, paired t-test, p=0.012). This weakening of synchronization is clearly shown in polar plots of the mean phase differences between oscillations in pairs of dINs (Fig. 7D). Power spectrum analysis showed that, with the weakening of synchronisation, the range of oscillation frequencies increased while peak frequencies significantly decreased (from 10.6 ± 2 Hz to 7.5 ± 1.3 Hz, n=10 dINs, paired t-test, $p<0.001$, Fig.7B). These results show that gap junctions play a significant role in synchronizing oscillations between coupled dINs, and presumably across the whole dIN population, and by doing so also increase and stabilise oscillation frequency (Soto-Trevino et al., 2005). There was an increase in oscillation amplitudes after 18-β-GA block (28.7 ± 11.4 mV to 38.8 ± 6.7 mV, paired-t-test, p=0.016), which could result from electrical coupling block. However, differences in oscillation amplitudes are very sensitive to average membrane potential levels (Fig.4C) and are also affected by the progress of amphotericin perforation of patch membrane at the beginning of recordings.

Swimming-like rhythms in hemi-CNS preparations

If the conditional pacemaker properties of dINs induced by NMDA play a role in the generation and maintenance of swimming activity then there are two predictions: firstly, swimming-like activity should be present when the inhibition that leads to post-inhibitory rebound firing in dINs is blocked (Soffe, 1989); secondly, swimming-like activity should be blocked by treatments which block NMDA induced dIN pacemaker properties (NMDAR antagonists and 0 Mg^{2+} saline). To test these predictions in hemi-CNS preparations we used 20 μM SR95531 and 1 μM Strychnine together to block GABA and glycine inhibition. To initiate swimming-like motor activity without application of NMDA, three or four 1 ms

current pulses at 30-40 Hz were applied to the hindbrain region (~7th rhombomere region). These stimuli evoked sustained rhythmic motor nerve bursts in all 10 hemi-CNS preparations tested (Fig. 8A, C; mean episode length: 5.3 ± 3.7 s, range: 1.4-21.1 s).These episodes were shorter than fictive swimming episodes seen in intact tadpoles. The frequency of motor nerve bursts fell quickly at the start of each episode (Fig. 8E). The average frequency was 20.6 ± 0.8 Hz (5 tadpoles, 17 episodes), similar to that seen in the first 5 seconds in intact tadpole fictive swimming (19.1 ± 1.8 Hz, n = 6 tadpoles, 15 episodes, p=0.21, Fig.8F).

When 25 μM of the NMDAR antagonist D-AP5 was bath-applied for 5 minutes, these episodes of rhythmic motor nerve activity were shortened by 98.4 ± 2.4 % (mean episode length: 0.12 ± 0.19 s, p=0.002, paired t-test, n=5 tadpoles. Fig. 8A, B). There was partial recovery after washing for 15 minutes (mean episode length: 2.0 ± 2.3s; 29 ± 35.6%). Critically, the rhythmic activity was also significantly shortened by 90.6 ± 15.1 % when tadpoles were bathed in saline with 0 Mg^{2+} (mean episode length: 0.38 ± 0.39s; p=0.005, paired t-test, n=5 tadpoles, Fig. 8C, D) with partial recovery after washing for 10 minutes (63.9 ± 48.5%). These data suggest that both NMDAR activation and Mg^{2+} are important in the generation of rhythmic activity in the simplified hemi-CNS preparation in the presence of inhibitory blockers.

NMDA induced hemi-CNS rhythmicity

Direct recordings previously showed that, when active, dINs release glutamate to excite each other (Li et al., 2006). The above results have now shown that NMDAR activation by glutamate or NMDA can modulate the firing properties of these dINs making them able to fire repetitively at frequencies similar to rhythmic swimming and therefore to act as conditional pacemakers. In addition, our extracellular recordings from intact spinal cord and hemi-CNS preparations showed that swimming-like rhythmic activity, after removing inhibition, depended on NMDAR activation. To test our conclusion that the conditional pacemaker activity of dINs provides a mechanism for rhythm generation, we checked that direct microperfusion of NMDA onto a hemi-CNS preparation led to rhythm generation even when inhibition was blocked. This also allowed us to directly examine the activity of dINs during rhythmic activity and test the quality of the rhythm generated. 100 μM NMDA was microperfused onto the caudal hindbrain with inhibitory blockers (1 μM Strychnine and 20 μM SR-95531) in the saline. A suction electrode was placed on the caudal spinal cord to record spinal network activity. NMDA application resulted in reliable rhythmic activity which, unlike the responses to electrical stimulation described above (Fig. 8A, C), could persist as long as NMDA was present (tested up to 260 s) in 13 out of 13 tadpoles (> 300 trials, Fig. 9A, C).

Whole-cell recordings were made from 9 dINs during NMDA-induced hemi-CNS rhythmic activity. All these dINs were depolarised and fired reliably throughout rhythmic network activity. Very often however (108/162 trials), rhythmic dIN firing began before the hemi-CNS rhythm consistent with it initiating the network rhythm. During hemi-CNS rhythmic activity dINs reliably fired a single spike in phase with each rhythmic s.c. burst (Fig. 9A). In contrast, recordings from 22 non-dIN interneurons showed a different form of response in that most (7 of 7 motoneurons, 11 of 15 non-dINs) responded to microperfused NMDA with a relatively weak depolarisation (6 ± 3.89 mV, range = 0 −15 mV) and never fired until the whole spinal cord network had become active (n = 191 trials, Fig. 9C). The remaining 4 non-dINs belonging to the two types of inhibitory interneuron in the swimming circuit sometimes (14 in 26 trials) responded to NMDA with a stronger depolarization and occasional firing (5-38 Hz, not illustrated).

The whole cell recordings, which suggest that firing occurs exclusively in dINs prior to the onset of hemi-CNS rhythmic activity and show that they fire reliably throughout rhythmic activity, again focussed attention on the central role of the dINs. If conditional pacemaker activity in dINs was driving the hemi-CNS rhythm, we might expect that the quality of rhythm (stability and consistency) would be stronger in the dINs than in other neurons. On the other hand, we might expect the quality to be less strong than in the intact tadpole with inhibition and therefore post-inhibitory rebound firing present. To address these questions, we used the coefficient of rhythmicity (see Methods) to assess the quality of fictive swimming generated following sensory stimulation in the intact tadpole and the swimming-like rhythms in the hemi-CNS in response to NMDA. This comparison appears reasonable given that the frequencies of spinal cord rhythms in the hemi-CNS induced by NMDA microperfusion (21.1 ± 3.3 Hz, n = 7 tadpoles), were very similar to those in the first 5 seconds of fictive swimming in intact tadpoles without inhibitory blockers (p=0.73).

We first compared the coefficient of rhythmicity (Cr) of spikes in individual whole-cell recordings and Cr of motor nerve bursts (monitoring motor output) in intact tadpoles. These were then compared with similar measurements in hemi CNSs without inhibition. The value of Cr for dIN firing in the intact tadpole was very high (1.00, n = 6). Values for non-dINs and for motor nerve activity in the intact animals were almost as high (0.94 ± 0.07 and 0.98 ± 0.01; n = 6 tadpoles analyzed). Surprisingly, values of Cr for dIN firing in hemi-CNS rhythms induced by NMDA were also very high, even in the presence of inhibitory blockers and therefore in the absence of PIR (1.0, n = 6). In contrast, the values for non-dINs and for spinal cord bursts (monitoring network activity) in the hemi-CNS were significantly lower (0.61 ± 0.16, n = 18 non-dINs, and 0.70 ± 0.16, n = 7 tadpoles, see above, $p<0.01$). This reduction in the quality of the motor rhythm compared to the firing of dINs was not surprising given that the blockers were likely to have removed precise inhibitory timing information.

Overall these results together with those of the previous section indicate that, in the presence of normal extracellular Mg^{2+} and with inhibition removed, NMDA activation alone can be sufficient to induce and maintain rhythmic activity in dINs which drives rhythmic activity in the whole spinal cord motor network.

NMDA-induced conditional pacemaker activity of dINs not only appears to provide an additional mechanism for rhythm generation within each side of the CNS, and not requiring inhibition, but it can produce rhythmic activity equivalent to that seen during swimming in the intact animal. It should therefore be possible to simply remove inhibition from an intact CNS and reveal independent rhythms on the two sides. To test this, we applied 30-50 μM NMDA to a ~700 μm length of spinal cord isolated by transecting at the 3rd and 7th post otic segments and removed inhibition by using 1 μM strychnine and 10-20 μM SR95531 or 20 μM bicuculline (diagram Fig. 10A). Soon after introducing the inhibitory blockers, NMDA application induced rhythmic swimming activity which alternated between the two sides (mean frequency 22.9 ± 5.2 Hz, n = 5 animals; Fig. 10B). Left-right coupling then became lost indicating a significant reduction of inhibition between the two sides. Despite this, rhythmic activity continued independently on each side at similar frequencies (right side: 22.4 ± 3.1 Hz; left side: 22.8 ± 3.7 Hz; Fig. 10C, D). These independent rhythms were presumably not due to post-inhibitory rebound but were most plausibly due to conditional pacemaker activity in spinal cord members of the dIN populations on each side of the CNS. In support of this, it has already been shown that little rhythm can be generated in the spinal cord by applied NMDA when in 0 mM Mg^{2+} (Soffe and Roberts, 1989).

Discussion

This paper describes a novel type of ionotropic receptor mediated self-resetting within a defined population of brainstem neurons. Intrinsic modulation of neuronal and synaptic network properties by other network members occurs in invertebrates (Katz and Frost, 1996; Sakurai and Katz, 2003), mediated by neuromodulators such as serotonin or peptides and can be state-dependent, altering according to pre and post-synaptic activity. Intrinsic modulation has also been described in vertebrates, primarily involving metabotropic transmitter receptors (e.g. mGluRs: (El Manira et al., 2002; Lieske and Ramirez, 2006; Chapman et al., 2008)). However, here we describe a self-resetting role for ionotropic NMDA receptors. We have shown that the agonist NMDA or the likely transmitter L-glutamate, can transform the reticulospinal dIN neurons that drive tadpole swimming (Li et al., 2006; Soffe et al., 2009) into pacemakers that fire repetitively within the swimming frequency range. With spiking blocked, NMDA application produces oscillations in these neurons at similar frequencies. Since dINs synapse with each other and release glutamate to activate NMDARs (Li et al., 2006), they can modulate the firing properties of their own population, specifically while in an active state. This targeted self-resetting allows one particular neuron type, the excitatory dIN neurons driving swimming, to be transformed rapidly (equivalent to a few swimming cycles) into pacemaker mode only while rhythm generation is occurring. One consequence is that the pacemaker properties of neurons during activity are not revealed when studied at rest.

Many rhythm generating networks controlling movement comprise symmetrical half centres coupled by reciprocal inhibition (Arshavsky et al., 1993; Marder et al., 2005; Feldman and Del Negro, 2006; Marder and Bucher, 2007; Brocard et al., 2010). Inhibition may play a role in rhythm generation but many networks can operate without it (Droge and Tao, 1993; Cowley and Schmidt, 1995; Ozaki et al., 1996; Kremer and Lev-Tov, 1997; Rioult-Pedotti, 1997; Stein et al., 1998; Cui et al., 2004; Cangiano and Grillner, 2005; Cui et al., 2005; Samara and Currie, 2008). The new self-resetting mechanism we describe provides one mechanism to explain this. The simple CPG network for tadpole swimming only contains dINs, two types of glycinergic inhibitory interneurons and motoneurons, greatly facilitating analysis of rhythm generation (Roberts et al., 2008). The current "*emergent network*" hypothesis is based on network connections where dINs feed back glutamate excitation, depolarise each other by activating NMDARs and then fire on rebound following reciprocal inhibition from the other side of the CNS (Li et al., 2006; Roberts et al., 2008; Soffe et al., 2009). With inhibition blocked pharmacologically and by removing one side of the CNS, some rhythm remained (Kahn and Roberts, 1982; Soffe, 1989). This suggested that pacemaker neurons were present but they remained elusive, even though the hemi-CNS with inhibition blocked simplified the CPG network to just dINs and motoneurons. Based on *in situ* whole-cell recordings, *Xenopus* tadpole swimming CPG neurons were proposed to be conditional oscillators because they could fire repetitively (Aiken et al., 2003). However, our much larger sample of recordings showed that most CPG neurons either fire repetitively at much higher frequencies than the normal swimming range (Sautois et al., 2007) or singly (dINs) to current injections (Li et al., 2006). Little evidence supported the conditional oscillator proposal. Our present results show that dINs are transformed by NMDAR activation into pacemakers, firing at frequencies seen during swimming. In contrast, NMDA application has little effect on the high frequency firing of other spinal CPG interneurons. Because only dINs fire at swimming frequencies during NMDAR activation and because they provide the excitatory input onto motoneurons, they are the clear candidates to drive hemi-CNS rhythms following either NMDA application or hindbrain stimulation. The hatchling *Xenopus* tadpole swimming CPG therefore uses a curious new mechanism, self-resetting, to allow rhythm generation without inhibition.

What is the role of NMDAR dependent oscillations in rhythmic systems? The oscillations we have described in tadpole dINs, in TTX, could directly drive their NMDAR-induced pacemaker firing, as suggested by their similar (~10 Hz) frequencies. However, it is more likely that the currents responsible for the oscillations normally interact with fast spike currents and fast ligand-gated synaptic currents in a more complex way to influence dIN rhythmic firing during swimming, perhaps stabilizing and constraining the frequency range. Since dINs appear to be the only tadpole spinal neurons showing fast, NMDA-induced oscillations (those described from presumed motoneurons by Prime, 1999, may actually have been from dINs), it should be possible to discover their role. This is important given the compelling evidence that hindbrain and spinal dINs provide the synaptic excitation that drives tadpole swimming (Li et al., 2006; Soffe et al., 2009). The functional significance of the much slower (≤ 1 Hz) NMDA induced, TTX-resistant oscillations reported in other animals, from neurons including spinal motoneurons and some interneurons, remains unclear. In motoneurons of lamprey, frog tadpoles and adult frogs (Grillner and Wallen, 1985; Wallen and Grillner, 1985, 1987; Sillar and Simmers, 1994; Rioult-Pedotti, 1997; Reith and Sillar, 1998; Prime et al., 1999), oscillation frequencies are somewhat slower than the locomotor rhythm. In motoneurons of turtles (Guertin and Hounsgaard, 1998) and mammals (Hochman et al., 1994b; MacLean et al., 1997; Tresch and Kiehn, 2000) oscillation frequencies are closer to those during fictive locomotion. However, it is uncertain whether the motoneurons are necessary for rhythm generation (Cowley et al., 2005), since motoneurons are not generally considered part of vertebrate CPGs, or whether the oscillatory mechanisms help pattern motoneuron firing (Brocard et al., 2010). In neonatal rat, slow (≤ 1Hz) TTX-resistant, NMDA- induced oscillations are seen in interneurons lying around the central canal (Hochman et al., 1994a). Some of them may be counterparts to Hb9-positive glutamatergic neurons in mice (Wilson et al., 2005; Ziskind-Conhaim et al., 2008), which are possible components of the spinal rhythm generating network (Brownstone and Wilson, 2008; Kwan et al., 2009; Brocard et al., 2010). Faster TTX-resistant, NMDA-induced oscillations seem less common but are found in some interneurons surrounding the neonatal rat central canal (Hochman et al., 1994a), as well as some adult *Xenopus* spinal motoneurons (Rioult-Pedotti, 1997), hippocampal pyramidal cells (Ganong and Cotman, 1986) and midbrain dopaminergic neurons (Deister et al., 2009). However, their roles are not known.

In this study we have shown that Mg^{2+} is necessary for the NMDA induced, TTX-resistant dIN oscillations, repetitive dIN firing, and hemi-CNS rhythms when inhibition was blocked. However, without Mg^{2+} dINs do not fire to slow depolarisations and only fire once at the onset of depolarising current injections even when NMDA is present. Experiments in TTX have shown that Mg^{2+} in some way promotes the generation of membrane potential oscillations, presumably by voltage-dependent blocking and unblocking of NMDARs but the role of other currents (like Ca^{2+} dependent K^{+}) is not yet clear. When dINs act as pacemakers to drive hemi-CNS rhythms, similar mechanisms are presumably operating but remain to be investigated. The role for Mg^{2+} here may be more complicated because Mg^{2+} can also block other currents like L-type calcium currents (Kuo and Hess, 1993). In lamprey, it has been proposed that Ca^{2+}-dependent K^{+} currents, low-voltage activated Ca^{2+} currents and Na^{+} dependent K^{+} currents could interact with TTX-resistant NMDA oscillations to mediate undulating motoneuron membrane potential changes during fictive swimming (see recent reviews (Grillner, 2003)). Investigation of such currents in *Xenopus* dINs is hampered by their mutual electrical coupling (Li et al., 2009) and the lack of satisfactory, coupling blockers. Electrical coupling is a feature of many other rhythm-generating networks and there is debate about whether it contributes to rhythm generation (see review refs (Kiehn and Tresch, 2002; Connors and Long, 2004)). In the tadpole significant block of electrical coupling desynchronises but does not stop NMDA induced oscillations, although it makes the normal swimming rhythm less reliable (Li et al., 2009). The coupling makes

direct investigation of the cellular mechanisms of oscillations difficult. For example, hyperpolarising a single dIN does not change oscillation frequency or block oscillations as it should in an uncoupled neuron (fig. 4C, D). If repolarisation depends on Ca^{2+}-dependent K^+ currents, then intracellular BAPTA injection might prevent it but oscillations can still spread in from other dINs. Transformation of dINs into pacemakers by NMDAR activation requires an inward current activated as the partial Mg^{2+} block becomes reduced by depolarisation, and then a repolarisation process following the spike. Other currents may contribute to pacemaker properties for example the persistent sodium current (I_{NaP}) identified in mammalian locomotor CPG neurons (Tazerart et al., 2008). All of this remains to be investigated.

In conclusion, our evidence shows that NMDA induced 10-25 Hz repetitive firing of excitatory reticulospinal neurons (dINs), in the presence of Mg^{2+}, can generate a swimming-like rhythm in both the half- and intact CNS when inhibition is blocked. This rapid intrinsic self-resetting acts exclusively between members of a single homogeneous population of excitatory premotor interneurons and is mediated by an ionotropic transmitter receptor. It may give the rhythm generating network additional robustness in life where many such networks have multiple rhythm generation mechanisms (Marder et al., 2005).

Acknowledgments

The research was funded firstly by a Wellcome Trust grant to Roberts and Soffe and then by a Royal Society University Research Fellowship to Li. Li carried out most experiments and data analyses. All three authors contributed to the conception and design of experiments, interpretation of data and manuscript writing. We thank Dr Matt Jones and Dr Marc Holderied for commenting on earlier versions of the paper.

References

Aiken SP, Kuenzi FM, Dale N. Xenopus embryonic spinal neurons recorded in situ with patch-clamp electrodes--conditional oscillators after all? Eur J Neurosci. 2003; 18:333–343. [PubMed: 12887415]

Arshavsky YI. Cellular and network properties in the functioning of the nervous system: from central pattern generators to cognition. Brain Res Rev. 2003; 41:229–267. [PubMed: 12663082]

Arshavsky YI, Orlovsky GN, Panchin YuV, Roberts A, Soffe SR. Neuronal control of swimming locomotion: analysis of the pteropod mollusc Clione and embryos of the amphibian Xenopus. Trends Neurosci. 1993; 16:227–233. [PubMed: 7688164]

Arshavsky, Yu I.; Gelfand, IM.; Orlovsky, GN.; Pavlova, GA.; Popova, LB. Origin of signals conveyed by the ventral spino-cerebellar tract and spino-reticulo-cerebellar pathway. Exp Brain Res. 1984; 54:426–431. [PubMed: 6723862]

Atsuta Y, Garcia-Rill E, Skinner RD. Characteristics of electrically induced locomotion in rat in vitro brain stem-spinal cord preparation. J Neurophysiol. 1990; 64:727–735. [PubMed: 2230919]

Brocard F, Tazerart S, Vinay L. Do pacemakers drive the central pattern generator for locomotion in mammals? Neuroscientist. 2010; 16:139–155. [PubMed: 20400712]

Brownstone RM, Wilson JM. Strategies for delineating spinal locomotor rhythm-generating networks and the possible role of Hb9 interneurones in rhythmogenesis. Brain Res Rev. 2008; 57:64–76. [PubMed: 17905441]

Buzsaki G, Draguhn A. Neuronal oscillations in cortical networks. Science. 2004; 304:1926–1929. [PubMed: 15218136]

Cangiano L, Grillner S. Fast and Slow Locomotor Burst Generation in the Hemispinal Cord of the Lamprey. J Neurophysiol. 2003; 89:2931–2942. [PubMed: 12611971]

Cangiano L, Grillner S. Mechanisms of Rhythm Generation in a Spinal Locomotor Network Deprived of Crossed Connections: The Lamprey Hemicord. J Neurosci. 2005; 25:923–935. [PubMed: 15673673]

Chapman RJ, Issberner JP, Sillar KT. Group I mGluRs increase locomotor network excitability in Xenopus tadpoles via presynaptic inhibition of glycinergic neurotransmission. Eur J Neurosci. 2008

Connors BW, Long MA. Electrical synapses in the mammalian brain. Annu Rev Neurosci. 2004; 27:393–418. [PubMed: 15217338]

Cowley KC, Schmidt BJ. Effects of inhibitory amino acid antagonists on reciprocal inhibitory interactions during rhythmic motor activity in the in vitro neonatal rat spinal cord. J Neurophysiol. 1995; 74:1109–1117. [PubMed: 7500136]

Cowley KC, Zaporozhets E, MacLean JN, Schmidt BJ. Is NMDA Receptor Activation Essential for the Production of Locomotor-Like Activity in the Neonatal Rat Spinal Cord? J Neurophysiol. 2005; 94:3805–3814. [PubMed: 16120672]

Cui WW, Saint-Amant L, Kuwada JY. shocked Gene Is Required for the Function of a Premotor Network in the Zebrafish CNS. J Neurophysiol. 2004; 92:2898–2908. [PubMed: 15212431]

Cui WW, Low SE, Hirata H, Saint-Amant L, Geisler R, Hume RI, Kuwada JY. The zebrafish shocked gene encodes a glycine transporter and is essential for the function of early neural circuits in the CNS. J Neurosci. 2005; 25:6610–6620. [PubMed: 16014722]

Deister CA, Teagarden MA, Wilson CJ, Paladini CA. An Intrinsic Neuronal Oscillator Underlies Dopaminergic Neuron Bursting. J Neurosci. 2009; 29:15888–15897. [PubMed: 20016105]

Droge MH, Tao Y. Glycine effects on in vitro motor pattern generation in mouse spinal cord. Neurosci Lett. 1993; 158:139–142. [PubMed: 8233086]

El Manira A, Kettunen P, Hess D, Krieger P. Metabotropic glutamate receptors provide intrinsic modulation of the lamprey locomotor network. Brain Res Rev. 2002; 40:9–18. [PubMed: 12589902]

Feldman JL, Del Negro CA. Looking for inspiration: new perspectives on respiratory rhythm. Nat Rev Neurosci. 2006; 7:232–242. [PubMed: 16495944]

Ganong AH, Cotman CW. Kynurenic acid and quinolinic acid act at N-methyl-D-aspartate receptors in the rat hippocampus. J Pharmacol Exp Ther. 1986; 236:293–299. [PubMed: 2867215]

Getting PA. Emerging principles governing the operation of neural networks. Annu Rev Neurosci. 1989; 12:185–204. [PubMed: 2648949]

Grillner S. The motor infrastructure: from ion channels to neuronal networks. Nat Rev Neurosci. 2003; 4:573–586. [PubMed: 12838332]

Grillner S, Wallen P. The ionic mechanisms underlying N-methyl-D-aspartate receptor-induced, tetrodotoxin-resistant membrane potential oscillations in lamprey neurons active during locomotion. Neurosci Lett. 1985; 60:289–294. [PubMed: 2415879]

Guertin PA. The mammalian central pattern generator for locomotion. Brain Res Rev. 2009; 62:45–56. [PubMed: 19720083]

Guertin PA, Hounsgaard J. NMDA-Induced intrinsic voltage oscillations depend on L-type calcium channels in spinal motoneurons of adult turtles. J Neurophysiol. 1998; 80:3380–3382. [PubMed: 9862937]

Harris-Warrick RM. Voltage-sensitive ion channels in rhythmic motor systems. Curr Opin Neurobiol. 2002; 12:646–651. [PubMed: 12490254]

Hochman S, Jordan LM, MacDonald JF. N-methyl-D-aspartate receptor-mediated voltage oscillations in neurons surrounding the central canal in slices of rat spinal cord. J Neurophysiol. 1994a; 72:565–577. [PubMed: 7983519]

Hochman S, Jordan LM, Schmidt BJ. TTX-resistant NMDA receptor-mediated voltage oscillations in mammalian lumbar motoneurons. J Neurophysiol. 1994b; 72:2559–2562. [PubMed: 7884484]

Kahn JA, Roberts A. Experiments on the central pattern generator for swimming in amphibian embryos. Phil Trans Roy Soc Lond B. 1982; 296:229–243. [PubMed: 17506220]

Kahn JA, Roberts A, Kashin SM. The neuromuscular basis of swimming movements in embryos of the amphibian Xenopus laevis. J Exp Biol. 1982; 99:175–184. [PubMed: 7130896]

Katz PS, Frost WN. Intrinsic neuromodulation: altering neuronal circuits from within. Trends Neurosci. 1996; 19:54–61. [PubMed: 8820868]

Kiehn O, Tresch MC. Gap junctions and motor behavior. Trends Neurosci. 2002; 25:108–115. [PubMed: 11814564]

Kremer E, Lev-Tov A. Localization of the Spinal Network Associated With Generation of Hindlimb Locomotion in the Neonatal Rat and Organization of Its Transverse Coupling System. J Neurophysiol. 1997; 77:1155–1170. [PubMed: 9084588]

Kuo CC, Hess P. Block of the L-type Ca2+ channel pore by external and internal Mg2+ in rat phaeochromocytoma cells. The Journal of Physiology. 1993; 466:683–706. [PubMed: 8410712]

Kwan AC, Dietz SB, Webb WW, Harris-Warrick RM. Activity of Hb9 interneurons during fictive locomotion in mouse spinal cord. J Neurosci. 2009; 29:11601–11613. [PubMed: 19759307]

Li W-C, Soffe SR, Wolf E, Roberts A. Persistent Responses to Brief Stimuli: Feedback Excitation among Brainstem Neurons. J Neurosci. 2006; 26:4026–4035. [PubMed: 16611819]

Li WC, Soffe SR, Roberts A. Spinal inhibitory neurons that modulate cutaneous sensory pathways during locomotion in a simple vertebrate. J Neurosci. 2002; 22:10924–10934. [PubMed: 12486187]

Li WC, Soffe SR, Roberts A. Glutamate and acetylcholine corelease at developing synapses. Proc Natl Acad Sci U S A. 2004; 101:15488–15493. [PubMed: 15494439]

Li WC, Roberts A, Soffe SR. Locomotor rhythm maintenance: electrical coupling among premotor excitatory interneurons in the brainstem and spinal cord of young Xenopus tadpoles. J Physiol. 2009; 587:1677–1693. [PubMed: 19221124]

Lieske SP, Ramirez JM. Pattern-specific synaptic mechanisms in a multifunctional network. II. Intrinsic modulation by metabotropic glutamate receptors. J Neurophysiol. 2006; 95:1334–1344. [PubMed: 16492945]

MacLean JN, Schmidt BJ, Hochman S. NMDA receptor activation triggers voltage oscillations, plateau potentials and bursting in neonatal rat lumbar motoneurons in vitro. Eur J Neurosci. 1997; 9:2702–2711. [PubMed: 9517475]

Marder E, Bucher D. Understanding circuit dynamics using the stomatogastric nervous system of lobsters and crabs. Annu Rev Physiol. 2007; 69:291–316. [PubMed: 17009928]

Marder E, Bucher D, Schulz DJ, Taylor AL. Invertebrate central pattern generation moves along. Curr Biol. 2005; 15:R685–699. [PubMed: 16139202]

Mayer ML, Westbrook GL, Guthrie PB. Voltage-dependent block by Mg2+ of NMDA responses in spinal cord neurones. Nature. 1984; 309:261–263. [PubMed: 6325946]

Nieuwkoop, PD.; Faber, J. Normal tables of Xenopus laevis (Daudin). Amsterdam; North Holland: 1956.

Noga BR, Kriellaars DJ, Jordan LM. The effect of selective brainstem or spinal cord lesions on treadmill locomotion evoked by stimulation of the mesencephalic or pontomedullary locomotor regions. J Neurosci. 1991; 11:1691–1700. [PubMed: 2045881]

Ozaki S, Yamada T, Iizuka M, Nishimaru H, Kudo N. Development of locomotor activity induced by NMDA receptor activation in the lumbar spinal cord of the rat fetus studied in vitro. Dev Brain Res. 1996; 97:118–125. [PubMed: 8946060]

Prime L, Pichon Y, Moore LE. N-Methyl-D-aspartate-induced oscillations in whole cell clamped neurons from the isolated spinal cord of Xenopus laevis embryos. J Neurophysiol. 1999; 82:1069–1073. [PubMed: 10444699]

Ramirez J-M, Tryba AK, Pena F. Pacemaker neurons and neuronal networks: an integrative view. Curr Opin Neurobiol. 2004; 14:665–674. [PubMed: 15582367]

Reith CA, Sillar KT. A role for slow NMDA receptor-mediated, intrinsic neuronal oscillations in the control of fast fictive swimming in Xenopus laevis larvae. Eur J Neurosci. 1998; 10:1329–1340. [PubMed: 9749787]

Rioult-Pedotti M. Intrinsic NMDA-Induced Oscillations in Motoneurons of an Adult Vertebrate Spinal Cord Are Masked by Inhibition. J Neurophysiol. 1997; 77:717–730. [PubMed: 9065844]

Roberts A, Li WC, Soffe SR, Wolf E. Origin of excitatory drive to a spinal locomotor network. Brain Res Rev. 2008; 57:22–28. [PubMed: 17825424]

Sakurai A, Katz PS. Spike timing-dependent serotonergic neuromodulation of synaptic strength intrinsic to a central pattern generator circuit. J Neurosci. 2003; 23:10745–10755. [PubMed: 14645466]

Samara RF, Currie SN. Electrically evoked locomotor activity in the turtle spinal cord hemi-enlargement preparation. Neurosci Lett. 2008; 441:105–109. [PubMed: 18597937]

Sautois B, Soffe SR, Li WC, Roberts A. Role of type-specific neuron properties in a spinal cord motor network. J Comput Neurosci. 2007; 23:59–77. [PubMed: 17237908]

Sillar KT, Simmers AJ. Electrical coupling and intrinsic neuronal oscillations in Rana temporaria spinal cord. Eur J Morphol. 1994; 32:293–298. [PubMed: 7803182]

Soffe SR. Roles of Glycinergic Inhibition and N-Methyl-D-Aspartate Receptor Mediated Excitation in the Locomotor Rhythmicity of One Half of the Xenopus Embryo Central Nervous System. Eur J Neurosci. 1989; 1:561–571. [PubMed: 12106115]

Soffe SR, Roberts A. The Influence of Magnesium Ions on the NMDA Mediated Responses of Ventral Rhythmic Neurons in the Spinal Cord of Xenopus Embryos. Eur J Neurosci. 1989; 1:507–515. [PubMed: 12106136]

Soffe SR, Roberts A, Li WC. Defining the excitatory neurons that drive the locomotor rhythm in a simple vertebrate: insights into the origin of reticulospinal control. J Physiol. 2009; 587:4829–4844. [PubMed: 19703959]

Soto-Trevino C, Rabbah P, Marder E, Nadim F. Computational model of electrically coupled, intrinsically distinct pacemaker neurons. J Neurophysiol. 2005; 94:590–604. [PubMed: 15728775]

Stein PSG, McCullough ML, Currie SN. Reconstruction of Flexor/Extensor Alternation during Fictive Rostral Scratching by Two-Site Stimulation in the Spinal Turtle with a Transverse Spinal Hemisection. J Neurosci. 1998; 18:467–479. [PubMed: 9412523]

Tazerart S, Vinay L, Brocard F. The persistent sodium current generates pacemaker activities in the central pattern generator for locomotion and regulates the locomotor rhythm. J Neurosci. 2008; 28:8577–8589. [PubMed: 18716217]

Thorn Perez C, Hill RH, El Manira A, Grillner S. Endocannabinoids mediate tachykinin-induced effects in the lamprey locomotor network. J Neurophysiol. 2009; 102:1358–1365. [PubMed: 19571197]

Tresch MC, Kiehn O. Motor coordination without action potentials in the mammalian spinal cord. Nat Neurosci. 2000; 3:593–599. [PubMed: 10816316]

Wallen P, Grillner S. The effect of current passage on N-methyl-D-aspartate-induced, tetrodotoxin-resistant membrane potential oscillations in lamprey neurons active during locomotion. Neurosci Lett. 1985; 56:87–93. [PubMed: 3892375]

Wallen P, Grillner S. N-methyl-D-aspartate receptor-induced, inherent oscillatory activity in neurons active during fictive locomotion in the lamprey. J Neurosci. 1987; 7:2745–2755. [PubMed: 3040925]

Wilson JM, Hartley R, Maxwell DJ, Todd AJ, Lieberam I, Kaltschmidt JA, Yoshida Y, Jessell TM, Brownstone RM. Conditional Rhythmicity of Ventral Spinal Interneurons Defined by Expression of the Hb9 Homeodomain Protein. J Neurosci. 2005; 25:5710–5719. [PubMed: 15958737]

Ziskind-Conhaim L, Wu L, Wiesner EP. Persistent sodium current contributes to induced voltage oscillations in locomotor-related hb9 interneurons in the mouse spinal cord. J Neurophysiol. 2008; 100:2254–2264. [PubMed: 18667543]

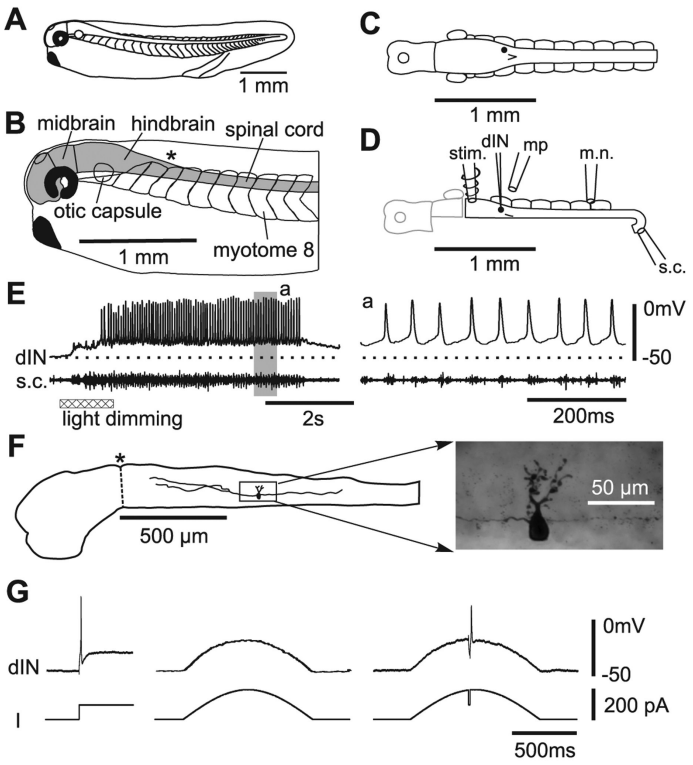

Figure 1.

Diagrams of the tadpole, experimental setup, activity during swimming and dIN anatomy. A. Tadpole at stage 37/38. B. Tadpole in a side view to show CNS (shaded). * marks caudal end of hindbrain. C. Top view of tadpole CNS and swimming myotomes, D. Hemi-CNS preparation. Electrodes and pipettes: stim., stimulation; dIN, whole-cell; mp, microperfusion; m.n., motor nerve; s.c., spinal cord. E. dIN activity during light-dimming evoked swimming-like rhythm recorded directly from the caudal spinal cord in normal saline. Dotted line in this and other figures indicates resting membrane potential. The record in the grey area (a) in this and other figures are expanded. F. Low power tracing of CNS from side showing the dIN in E and high power photo of the boxed area (same dIN as in Fig. 2C). Dashed line at asterisk separates midbrain and hindbrain. G. A dIN firing reliably at the onset of square current injections (left) fails to fire any spike to slowly rising depolarization (middle) but can fire following a reduction of slow sinusoidal current injection (I) for 25 ms.

Europe PMC Funders Author Manuscripts

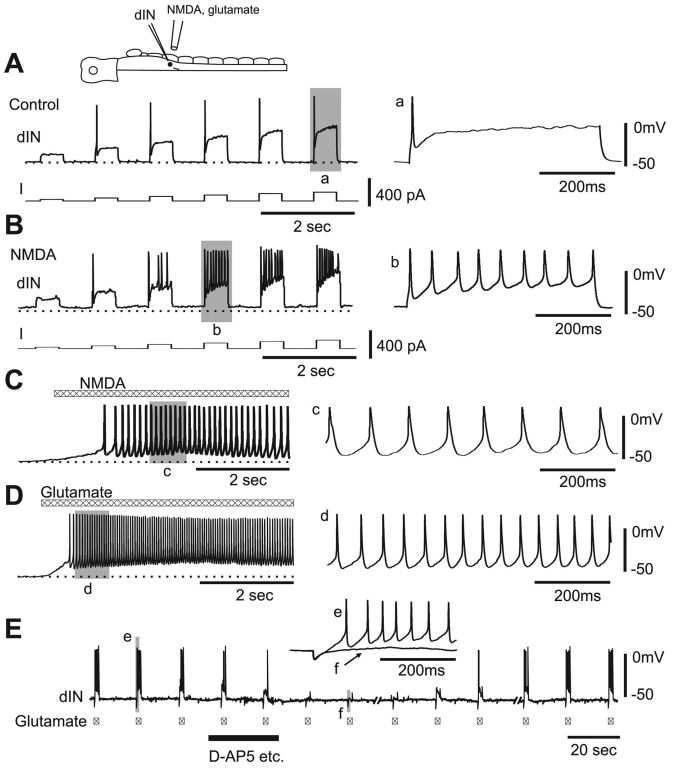

Figure 2.

dINs fire repetitively to NMDA and glutamate application. A. At rest, a dIN fires single action potentials to current injections. B. dIN in A fires repetitively when 100 μM NMDA applied by microperfusion depolarized the membrane potential by ~ 5 mV from rest (dotted line). C. Repetitive dIN firing response to microperfusion of NMDA alone. D. Another dIN fired repetitively to microperfusion of 1 mM glutamate. In C and D saline contained 1 μM strychnine, 20 μM SR95531, 5 μM NBQX, 2 μM DHβe and 150 μM Cd^{2+}. E. A dIN's responses to L-glutamate applied via a microiontophoresis electrode (−0.8 nA, ~ 20 microns away from dIN) before, during and after antagonist cocktail (D-AP5 etc: 50 μM D-AP5, 1 μM strychnine, 20 μM SR95531, 5 μM NBQX, 2 μM DHβe) dropped into a small well upstream to the recording chamber. Saline contained 150 μM Cd^{2+}. Shaded area records a, b, c, d, e and f are expanded on the right.

Europe PMC Funders Author Manuscripts

Europe PMC Funders Author Manuscripts

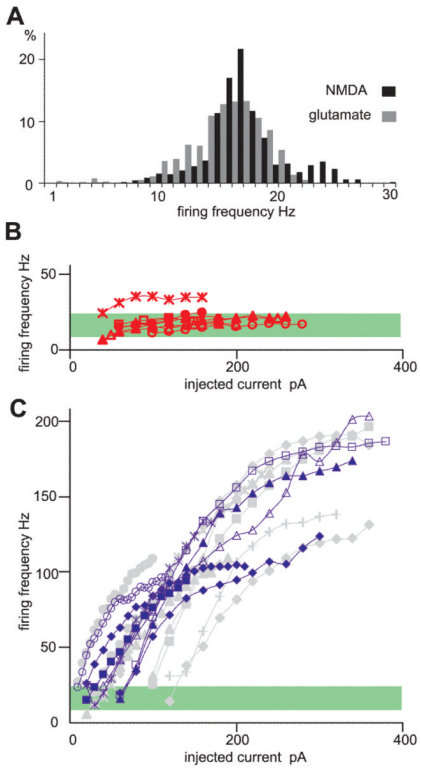

Figure 3.

The frequency range of NMDA induced firing. **A.** Comparison of dIN firing frequency distributions evoked by NMDA and glutamate applications in the presence of 1 μM strychnine, 20 μM SR95531, 2 μM DHβe, 5 μM NBQX and 150-200 μM Cd^{2+} (NMDA: 1192 spikes from 7 dINs; glutamate: 680 spikes from 5 dINs). Counts of spikes per frequency bin were normalised to percentages for each neuron and averaged across the sample. **B, C**. effects of current level on neuronal firing in the presence of NMDA in dINs (red symbols and lines in B) and non-dINs (blue in C). Grey symbols in C show non-dIN firing in control saline. Green area shows normal swim frequency range (10-25Hz).

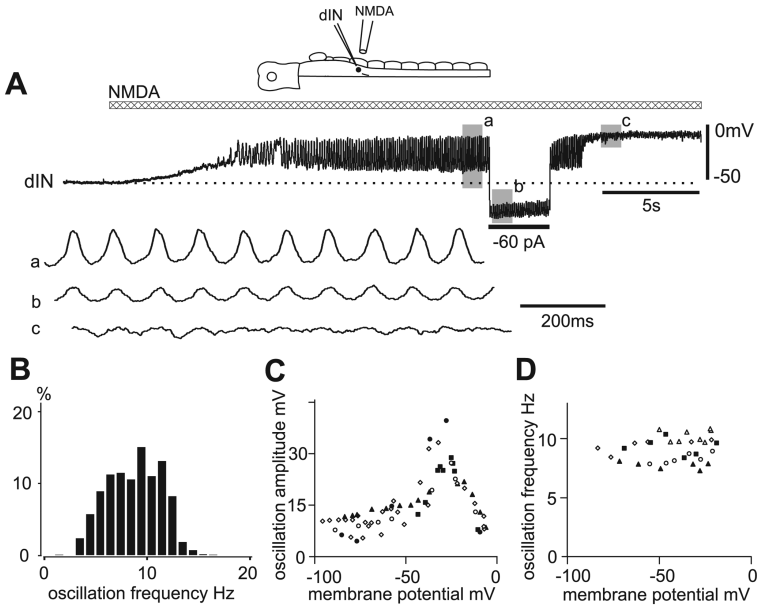

Figure 4.

NMDA induced dIN oscillations in TTX. A. Depolarisation and membrane potential oscillations in a dIN during NMDA application (bar) in TTX. Shaded areas a, b and c are expanded below to show oscillations. B. Frequency distribution of TTX-resistant oscillations in dINs evoked by microperfused NMDA (1589 cycles from 10 dINs). Counts of cycles per frequency bin were normalised to percentages for each neuron and averaged across the sample. C. The relationship between the amplitude of NMDA induced TTX-resistant oscillations and membrane potential changed by current injections. D. The relationship between oscillation frequency and half oscillation height membrane potential levels when NMDA was bath-applied. Different symbols indicate different dINs.

Europe PMC Funders Author Manuscripts

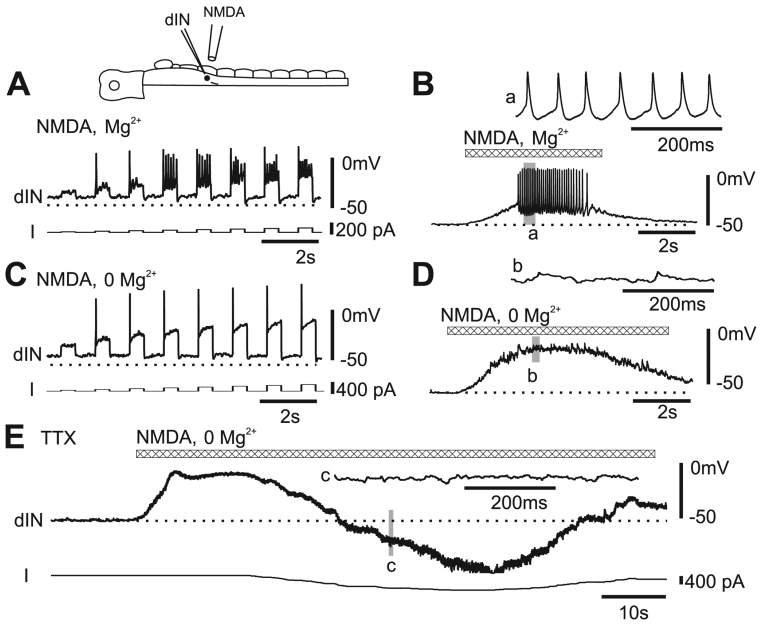

Figure 5.

Removal of Mg^{2+} from the saline abolished both NMDA induced repetitive firing and TTX-resistant oscillations in dINs. A, In saline containing Mg^{2+}, dIN fired repetitively to current injection during NMDA application. B, when NMDA leads to larger depolarisation, dIN also fires repetitively. C, When Mg^{2+} was removed from saline, the dIN only fired once to current injection during NMDA application. D, In 0 Mg^{2+} another dIN failed to fire any spikes when depolarized only by NMDA. E, In 0 Mg^{2+} and TTX, NMDA application did not evoke oscillations in a dIN even during negative current injection. a, b and c records are expanded.

Europe PMC Funders Author Manuscripts

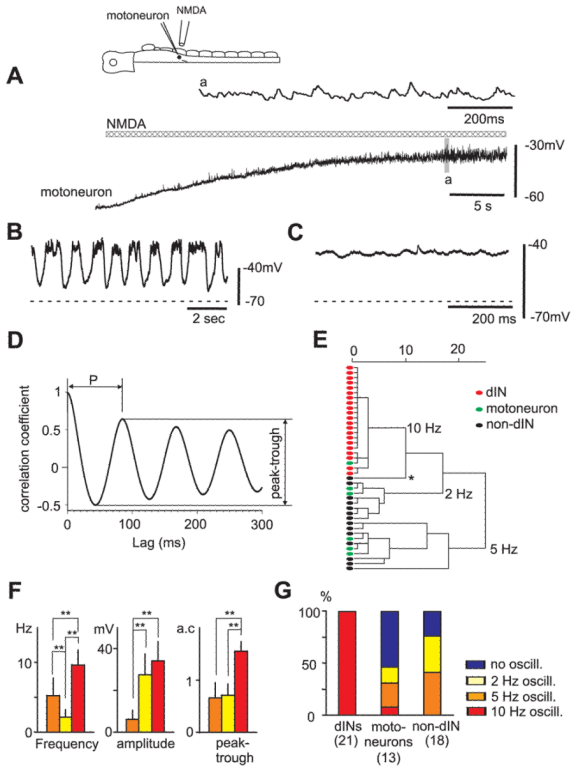

Figure 6.

Comparison of responses of dINs and non-dIN neurons active during swimming to NMDA in TTX. A. A motoneuron only produced depolarisation and increased noise. B. A non-dIN interneuron produced big, slow oscillations during NMDA evoked depolarisation. C, In another motoneuron there were only small ~10 Hz oscillations. Dashed lines indicate resting membrane potentials. D, Autocorrelation of oscillations during the current injection period in dIN in Fig 4A. The first autocorrelation peak period (P) and peak-trough difference are used for cluster analysis in E. E. Dendrogram of a cluster analysis result showing 3 clusters of neurons with oscillations at 10Hz, 2 Hz and 5 Hz. Asterisk marks the one non-dIN interneuron with high frequency unreliable big oscillations. F. Comparing the oscillation frequencies, amplitudes and autocorrelation peak-to-trough differences in the three clusters in E. G. The proportion of dINs, motoneurons and non-dIN interneurons with oscillatory responses. Colour coding in G also applies to F. For details see main text.

Europe PMC Funders Author Manuscripts

Europe PMC Funders Author Manuscripts

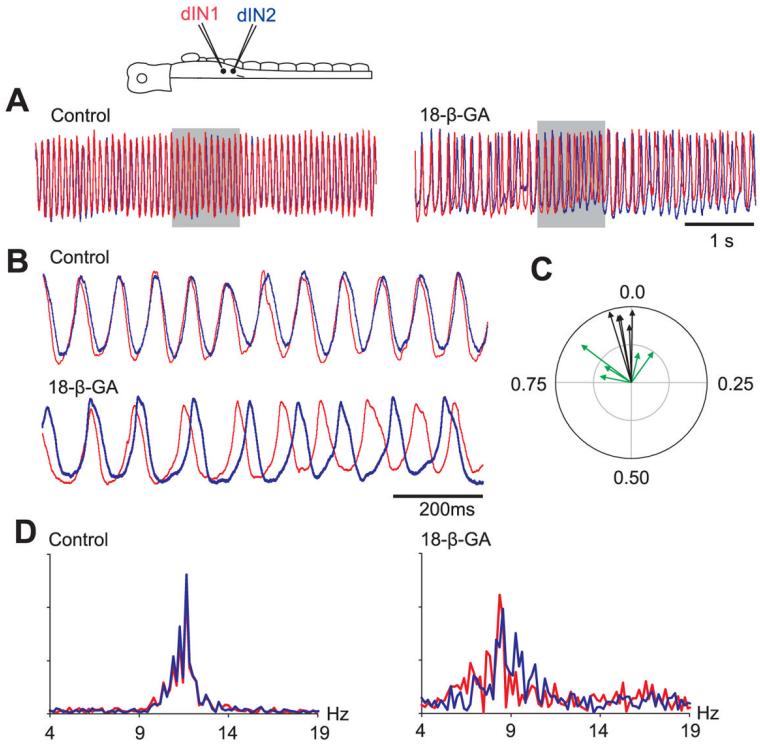

Figure 7.

Blocking gap junctions desynchronises the oscillations evoked by NMDA application in TTX. A. simultaneous recording from 2 dINs shows their oscillations in control and in 18-β-GA. B. De-synchronization of NMDA oscillations in 18-β-GA. Stretched 1 second oscillations marked by grey bars in A to show the synchrony of oscillation in the two dINs. Amplitudes of oscillations (blue from 25.4 in control to 39.8 mV, red 26.8 from to 39.2 mV) were normalised and records overlapped for easier comparisons in A and B. C. Polar plots of the mean relative phase of oscillations in 5 pairs of simultaneously recorded dINs before (black arrows) and after 18-β-GA application (green arrows, 5.5 seconds of oscillation analyzed in each record). D. Power spectrum of 5.5 seconds of oscillation in control and during the coupling block.

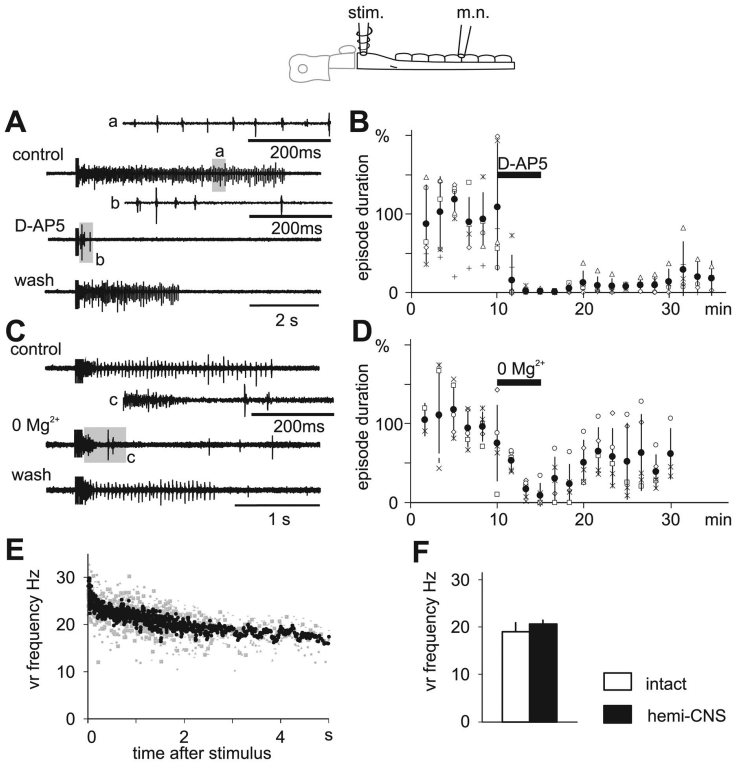

Figure 8.

Endogenous swimming-like activity in hemi-CNS without inhibition relies on NMDAR activation and Mg^{2+}. A. An examples of motor nerve (m.n.) records showing swimming-like activity episodes before, during and after D-AP5 application (25 μM, 5 minutes). B, Time series plots showing changes in episode durations during an experiment when hindbrain was stimulated every 100 seconds. C, D, Effect of 0 Mg^{2+} saline on swimming-like activity. E. Frequency of swimming-like vr activity in hemi-CNS after stimuli at time = 0. Grey symbols are from 17 episodes in 5 tadpoles and the black dots are moving averages. F. the hemi-CNS m.n. rhythm frequency is similar to that in the first 5 seconds that in intact tadpole fictive swimming. In A and C insets a, b and c show m.n. at expanded time scale.

Europe PMC Funders Author Manuscripts

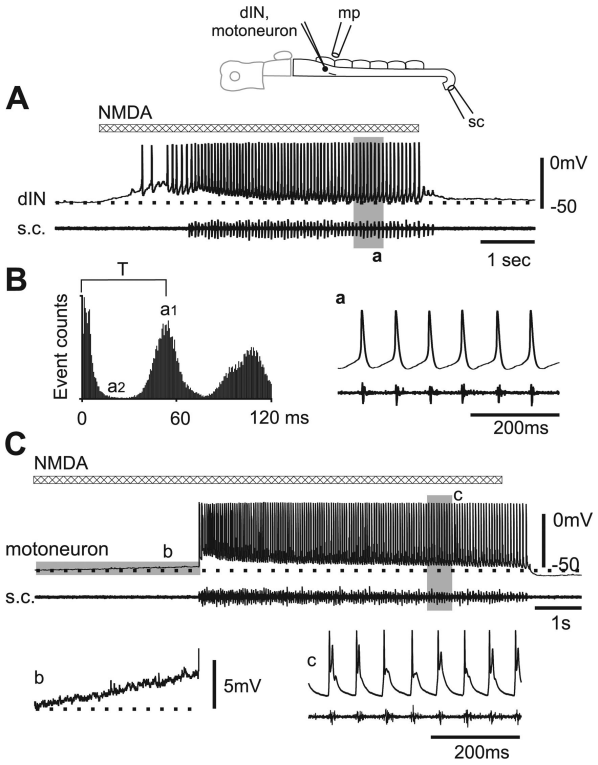

Figure 9.

Network activity in hemi-CNS induced by local microperfusion of NMDA onto the hindbrain in saline containing 1 μM Strychnine and 20 μM SR95531. A. dIN was depolarised and starts to fire before rhythmic sc activity starts. B. Distribution histogram of the intervals between sc burst triggered events in A. a1 and a2 are peak and trough counts respectively used for calculating coefficient of rhythmicity (Cr=0.99 for record in A). T is used for calculating rhythm frequency. C. A motoneuron was only slightly depolarised and starts to fire only when rhythmic s.c. activity starts.

Europe PMC Funders Author Manuscripts

Europe PMC Funders Author Manuscripts

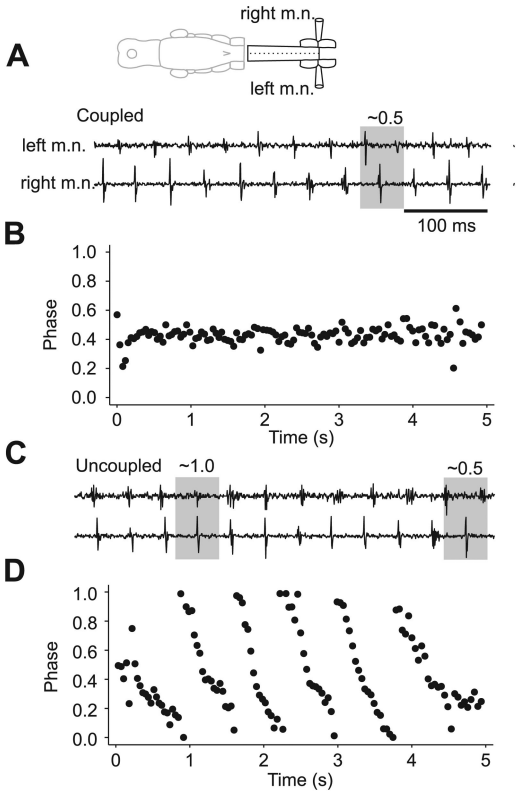

Figure 10.

Network activity in the spinal cord induced by bath perfusion of NMDA. A. Sustained swimming rhythm recorded from motor nerve (m.n.) on opposite sides of a ~700 μm length of spinal cord. B. Phase plot showing activity alternates between the two sides (also see shaded cycle in A). C. Rhythm continues despite phase uncoupling produced by 1 μM Strychnine and 20 μM SR9553. D. Phase plot for record in C.